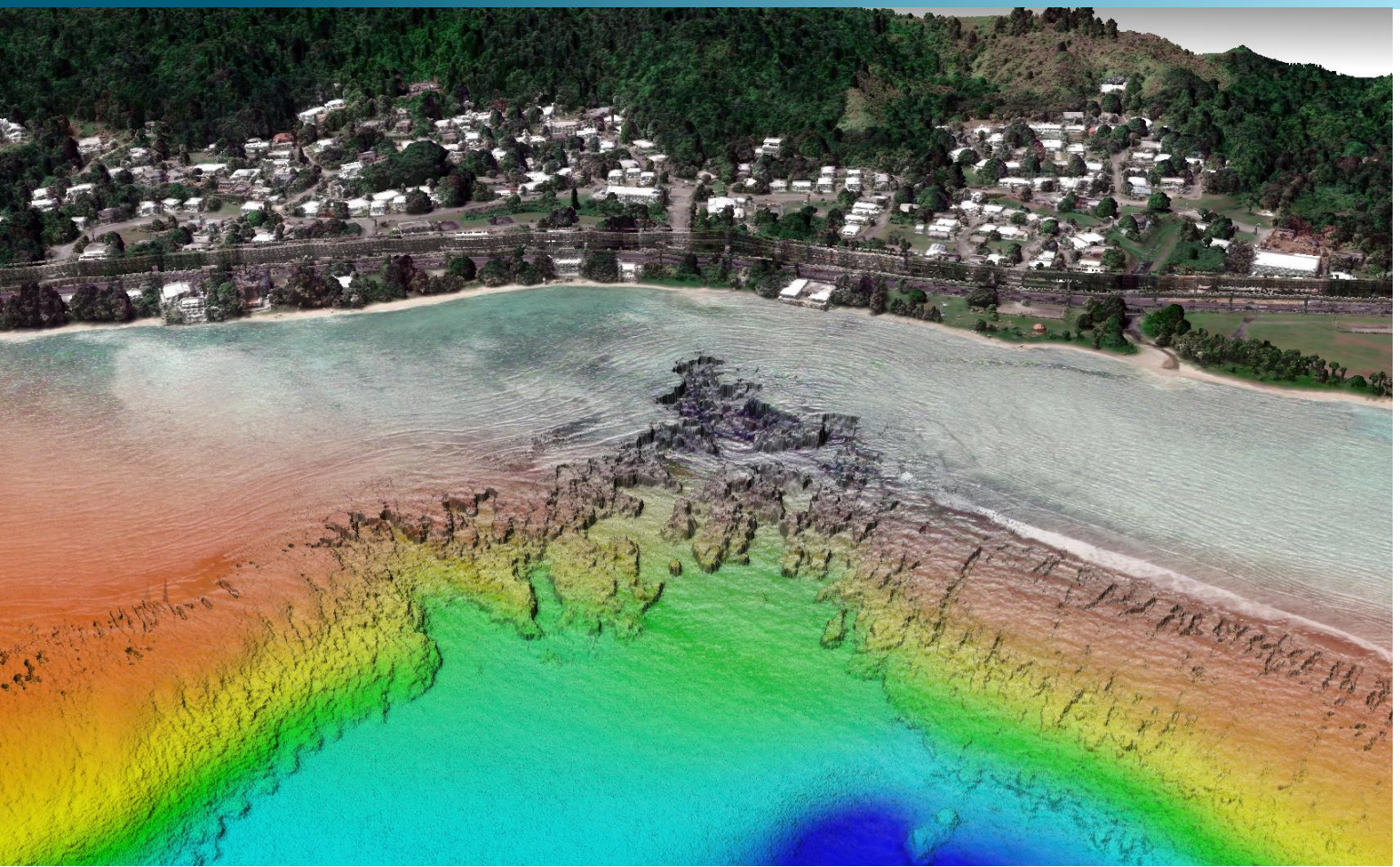


June 25, 2021



NOAA Typhoon Yutu Supplemental Mapping, Guam and CNMI

Supplemental Lidar & Shoreline Mapping GU1903-TB-C, MP1907-TB-C

Technical Data Report, NOAA Contract: EA-133C-14-CQ-0007, Task Order 1305M220FNCNL0053

Prepared For:



NOAA; National Geodetic Survey

Gregory Stinner
1315 East West Highway
Silver Spring, MD 20910
PH: 301-713-3167 ext.133

Prepared By:



NV5

1100 NE Circle Blvd, Ste. 126
Corvallis, OR 97330
PH: 301-713-3198

TABLE OF CONTENTS

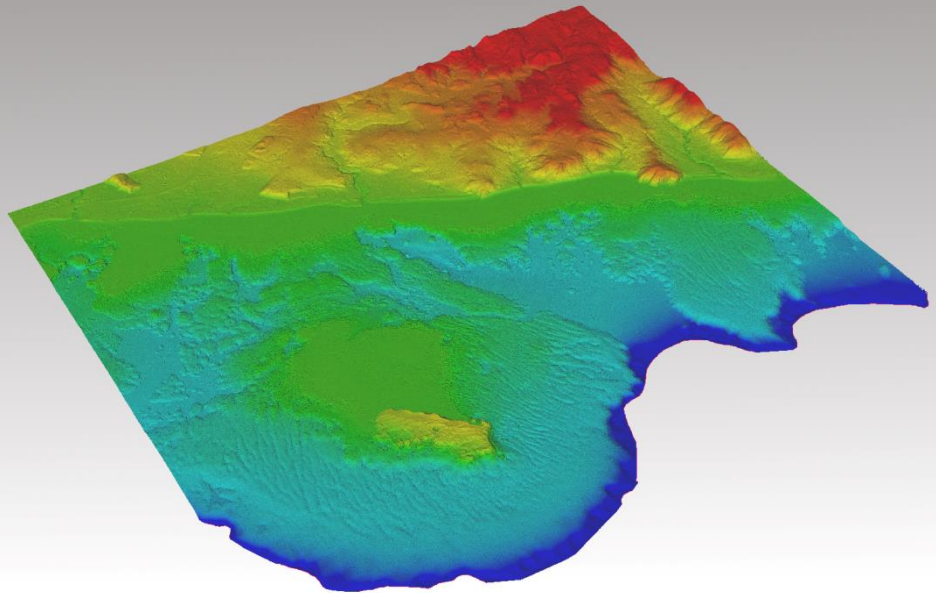
INTRODUCTION	1
Deliverable Products	2
Project Team.....	5
Lidar Survey Area	5
Shoreline Mapping Area.....	9
Lidar Deliverables	12
DEM Deliverables	12
Shoreline Deliverables	12
ACQUISITION	14
Planning.....	14
Lidar Survey	15
Ground Survey	17
Base Stations	17
Ground Survey Points (GSPs)	18
Aerial Targets	18
Land Cover Class.....	18
PROCESSING	21
Topobathymetric Lidar Data.....	21
Bathymetric Refraction	21
Lidar Derived Products.....	23
Topobathymetric DEMs	23
RESULTS & DISCUSSION	24
Bathymetric Lidar.....	24
Lidar Point Density	25
First Return Point Density	25
Bathymetric and Ground Classified Point Densities.....	25
Lidar Accuracy Assessments	27
Lidar Non-Vegetated Vertical Accuracy.....	27
Lidar Bathymetric Vertical Accuracies	30
Lidar Vegetated Vertical Accuracies	31
Lidar Relative Vertical Accuracy	33
Lidar Horizontal Accuracy	34

GLOSSARY	35
APPENDIX A - ACCURACY CONTROLS.....	37

Cover Photo: A view looking south at the Submarine Canyon on Asan point. The image was created from the Lidar bare earth model and lidar point cloud colored by elevation and RGB values from imagery respectively.

INTRODUCTION

This image shows Ana's Island in the foreground looking towards the southwestern shore of Guam within the Typhoon Yutu Supplemental Topobathymetric Lidar site . The image was made with a topobathymetric Lidar hillshade colored by elevation.



In January 2020, NV5 Geospatial (NV5) was contracted by the National Oceanic and Atmospheric Administration's (NOAA) National Geodetic Survey (NGS) Remote Sensing Division (RSD) Coastal Mapping Program (CMP), to collect topobathymetric Light Detection and Ranging (Lidar) data in the winter of 2020 into early summer for the Typhoon Yutu Supplemental sites on the Island of Guam as well as four islands in the Commonwealth of the Northern Marianas Islands (CNMI) (Alamagan, Anatahan, Sarigan, and Guguan) (Contract No. EA-133C-14-CQ-0007). Additionally, NV5 was contracted to provide shoreline mapping for the Island of Guam and six additional islands in the Commonwealth of the Northern Marianas Islands (CNMI) (Pagan, Farallon de Medinilla, Saipan, Tinian, Aguijan, and Rota.) Data were collected and completed to aid NOAA in assessing the topobathymetric surface of the near-shore and intertidal zones of the study area to support mapping and updating of the national shoreline.

The topobathymetric Lidar dataset was divided, processed, and delivered in two separate deliveries. The shoreline deliverables were divided, processed, and delivered in five separate deliveries. This report provides a comprehensive summary of the delivered topobathymetric lidar and shoreline compilation products. Documented herein are contract specifications, data acquisition procedures, processing methods, and accuracy results. Acquisition dates and acreage are shown in Table 1, a complete list of contracted deliverables provided to NOAA is shown in Table 2, and the project extents are shown in Figure 1 - Figure 7.

Table 1: Acquisition dates, acreage, and data types collected on the Typhoon Yutu Supplemental sites

Project Site	Contracted Acres	Buffered Acres	Acquisition Dates	Data Type
Typhoon Yutu Supplemental: Guam, Anatahan, Alamagan, Sarigan, and Guguan	178,751	185,000	01/20/2020 – 07/13/2020	Topobathymetric Lidar
Typhoon Yutu Supplemental Mapping: Guam, Pagan, Farallon de Medinilla, Saipan, Tinian, Aguijan, and Rota	641,374	641,374	N/A	Shoreline Mapping

Deliverable Products

Table 2: Products delivered to NOAA for the Typhoon Yutu Supplemental sites

Typhoon Yutu Supplemental Mapping Products	
Classified LAS Projection: UTM Zone 55 North Horizontal Datum: NAD83 (MA11) Vertical Datums: GRS80, GUV04 (GEOID12b) & NMVD03(GEOID12b) Units: Meters	DEM Projection: UTM Zone 55 North Horizontal Datum: NAD83 (MA11) Vertical Datums: GUV04 (GEOID12b) & NMVD03(GEOID12b) Units: Meters
Points	LAS v 1.4, Point Format 6 – Ellipsoidal & Orthometric Heights <ul style="list-style-type: none"> All Classified Returns, with Depth Bias Correction for Depth
Rasters	1 Meter ERDAS Imagine Files (*.img) <ul style="list-style-type: none"> Void Clipped Topobathymetric Bare Earth Digital Elevation Model (DEM) Topobathymetric Standard Deviation 1 Meter GeoTiffs (*.tif) <ul style="list-style-type: none"> DZ Orthos
Vectors	Shapefiles (*.shp) <ul style="list-style-type: none"> Project Boundary Lidar Tile Index DEM Tile Index Bathymetric Void Shape Flightline Index Flight Date Coverage Polygon

Shoreline Mapping	Shapefiles (*.shp) <ul style="list-style-type: none"> Segmented Mean High Water Shoreline Segmented Mean Lower Low Water Shoreline
Reports	<ul style="list-style-type: none"> Ground Survey Report (<i>Yutu Supplemental Ground Control Report.pdf</i>) LiDAR QC Reports per Delivery (<i>NOAA_Typhoon_Yutu_Guam_Cover_Letter.pdf</i> - <i>NOAA_Typhoon_Yutu_CNMI_Cover_Letter.pdf</i>) Final Compiled Report of Survey FGDC Compliant Metadata Airborne Collection Log and Lift Extents/Coverage Airborne Navigation and Kinematic GPS Reports Airborne Positioning and Orientation Reports Boresight Calibration Report Shoreline Mapping Project Completion Reports (<i>QSI Project Completion Report GU1903.pdf</i> & <i>QSI Project Completion Report MP1907A-D.pdf</i>) Additional Reports (<i>QSI_Guam_SurveyReport-r0.pdf</i>)

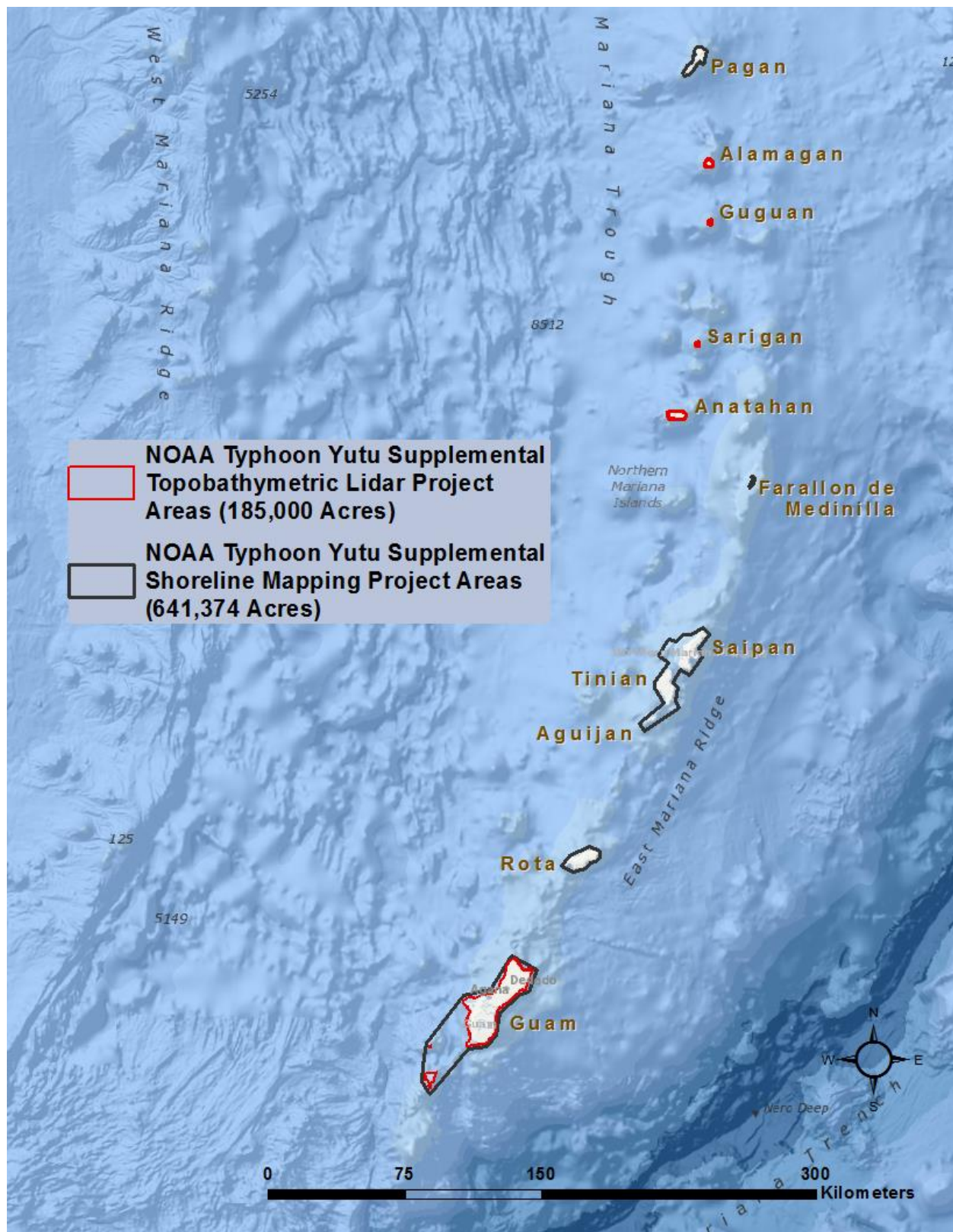


Figure 1: Location map of the full NOAA Typhoon Yutu Supplemental Shoreline Mapping and Topobathymetric Lidar Project Areas in Micronesia.

Project Team

NV5 served as the prime contractor for the NOAA Typhoon Yutu project. Woolpert, Inc. a subcontractor to NV5, completed all ground control acquisitions, lidar acquisitions and processing including lidar extraction, calibration and refraction, and editing. Woolpert, Inc. generated all deliverable Digital Elevation Models (DEM), raster layers, and lidar-derived void polygons from processed lidar data. NV5 provided the final quality control checks on delivered data, completed the LAS headering process, final assessments of vertical and horizontal accuracies.

NOAA's National Geodetic Survey team derived the initial shoreline files from the final delivered topobathymetric lidar data, and provided them to NV5 for editing and attribution. All shoreline editing and deliverables were completed by NV5's St. Petersburg office.

Lidar Survey Area

The Typhoon Yutu Supplemental Topobathymetric Lidar project area was contracted to cover approximately 279 square miles in the Micronesia region of the Pacific Ocean. The Typhoon Yutu Lidar area includes the four Commonwealth of the Northern Mariana Islands of Alamagan, Guguan, Sarigan, and Anatahan, the Island of Guam, and includes a portion of the Galvez Banks seamount. NV5 subcontracted Woolpert, Inc. to conduct all lidar acquisition and lidar processing of the project area between January 20th, 2020 and July 13th, 2020.

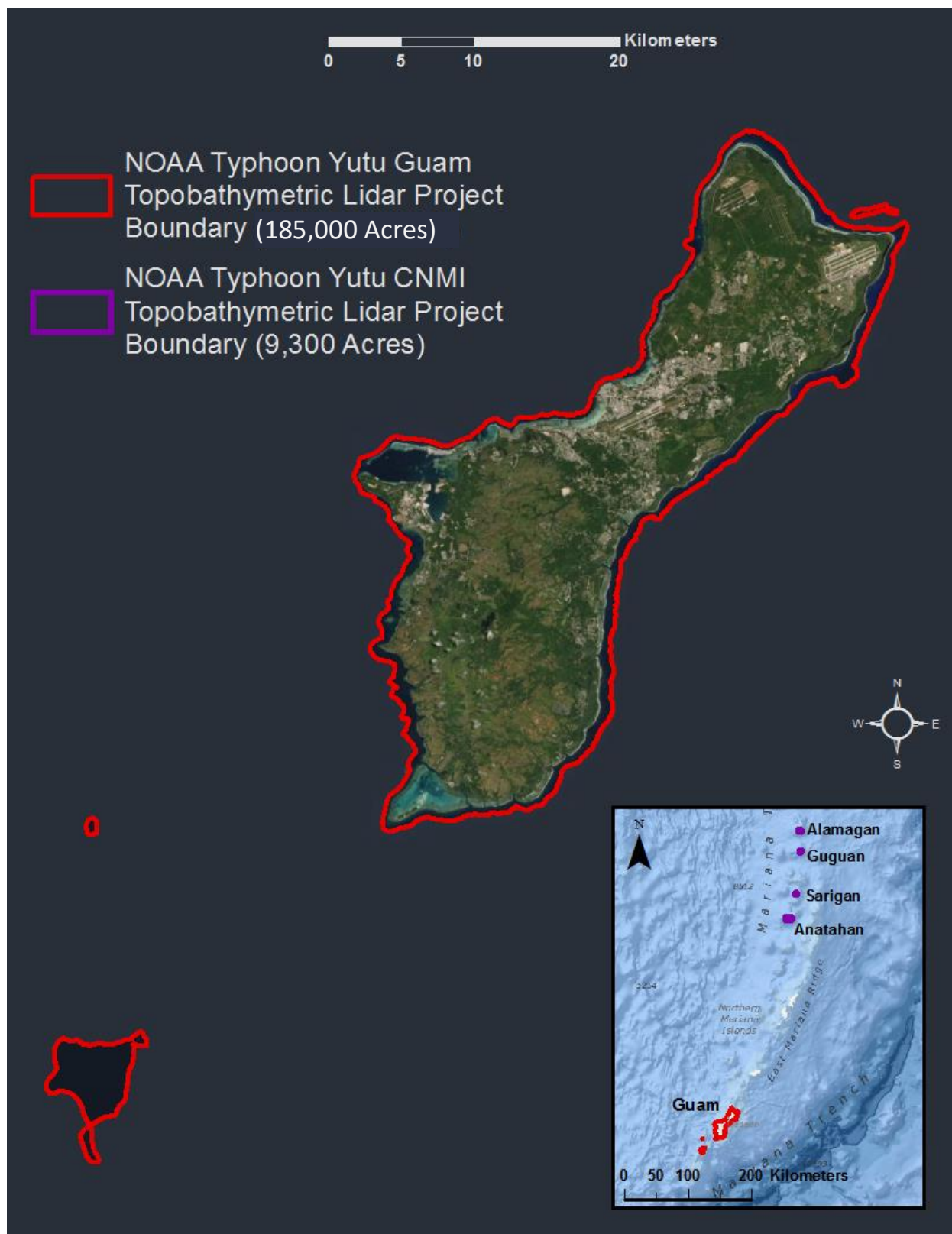


Figure 2: Location map of the Typhoon Yutu Supplemental Topobathymetric Lidar Guam site.



Figure 3: Location map of the Typhoon Yutu Supplemental Topobathymetric Lidar CNMIs Alamagan and Guguan sites.

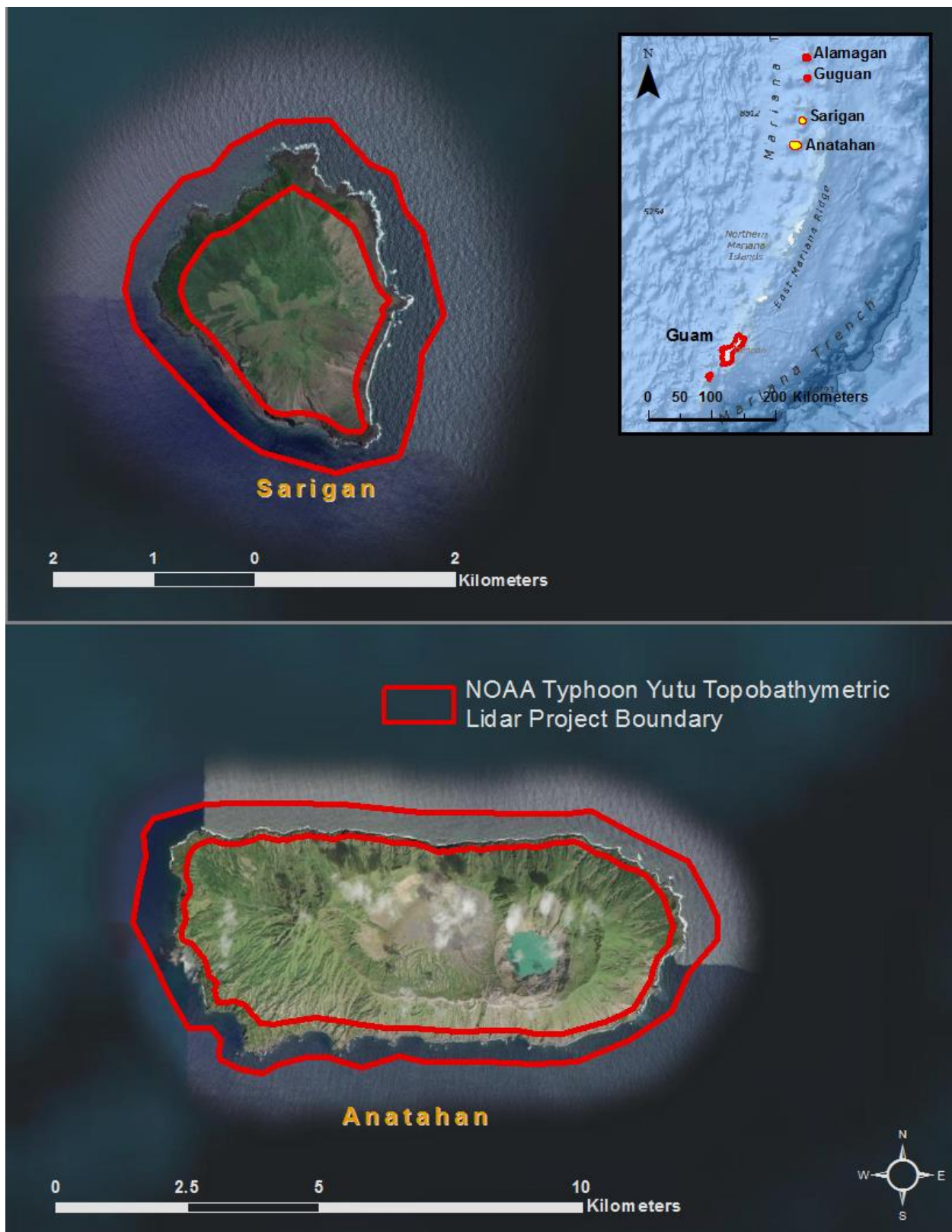


Figure 4: Location map of the NOAA Typhoon Yutu Supplemental Topobathymetric Lidar CNMIs Sarigan and Anatahan sites

Shoreline Mapping Area

The Typhoon Yutu Supplemental Topobathymetric Shoreline Mapping project area was contracted to cover approximately 1,002 square miles in the Micronesia region of the Pacific Ocean. The Typhoon Yutu Shoerline Mapping areas includes the six Commonwealth of the Northern Mariana Islands of Pagan, Farallon de Medinilla, Sapian, Tinian, Aguijan, and Rota, as well as the Island of Guam, and a portion of the Galvez Banks seamount. NV5 Geospatial's St. Petersburg office completed all shoreline mapping.

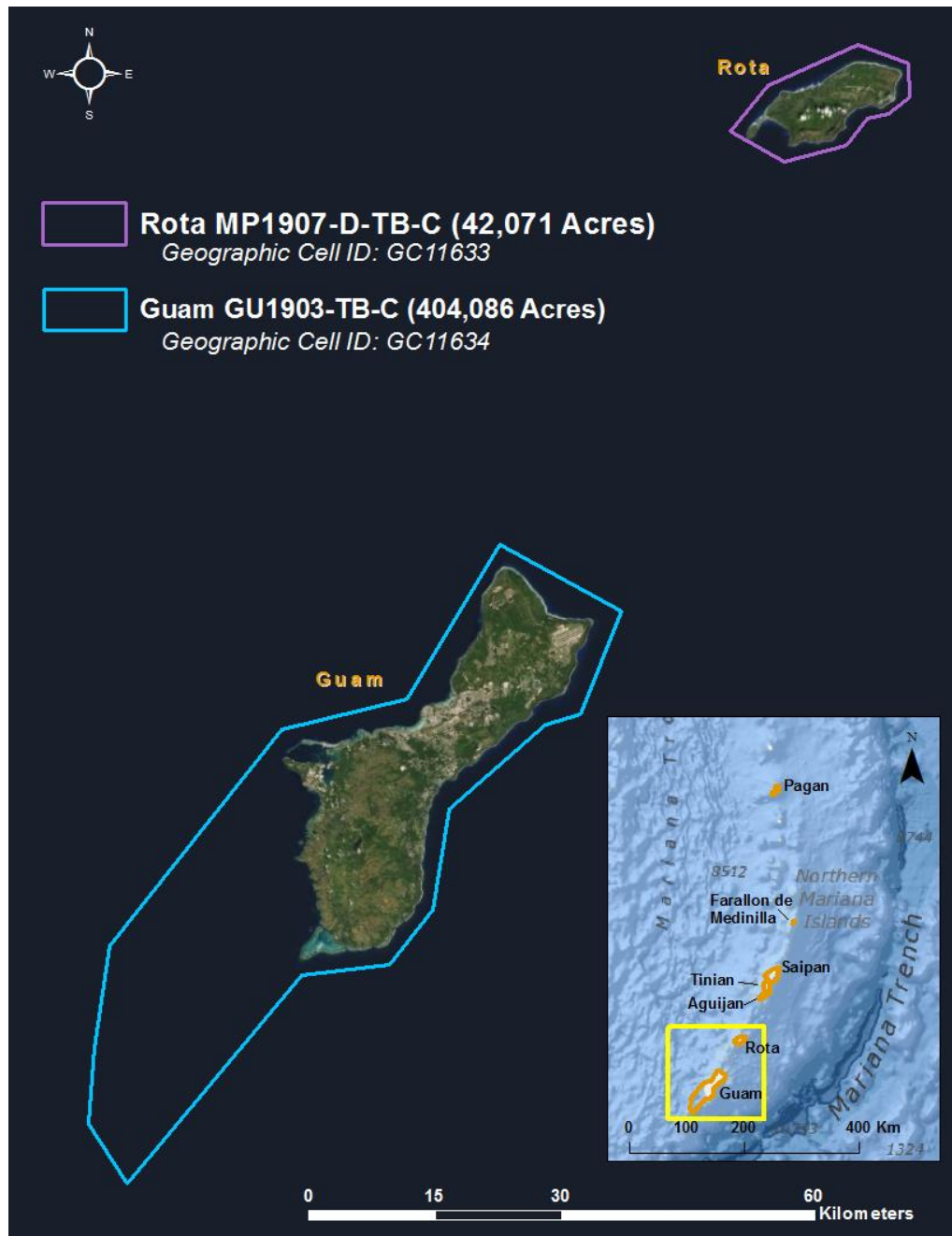


Figure 5: Location map of the Typhoon Yutu Supplemental Shoreline Mapping sites of Guam and Rota.

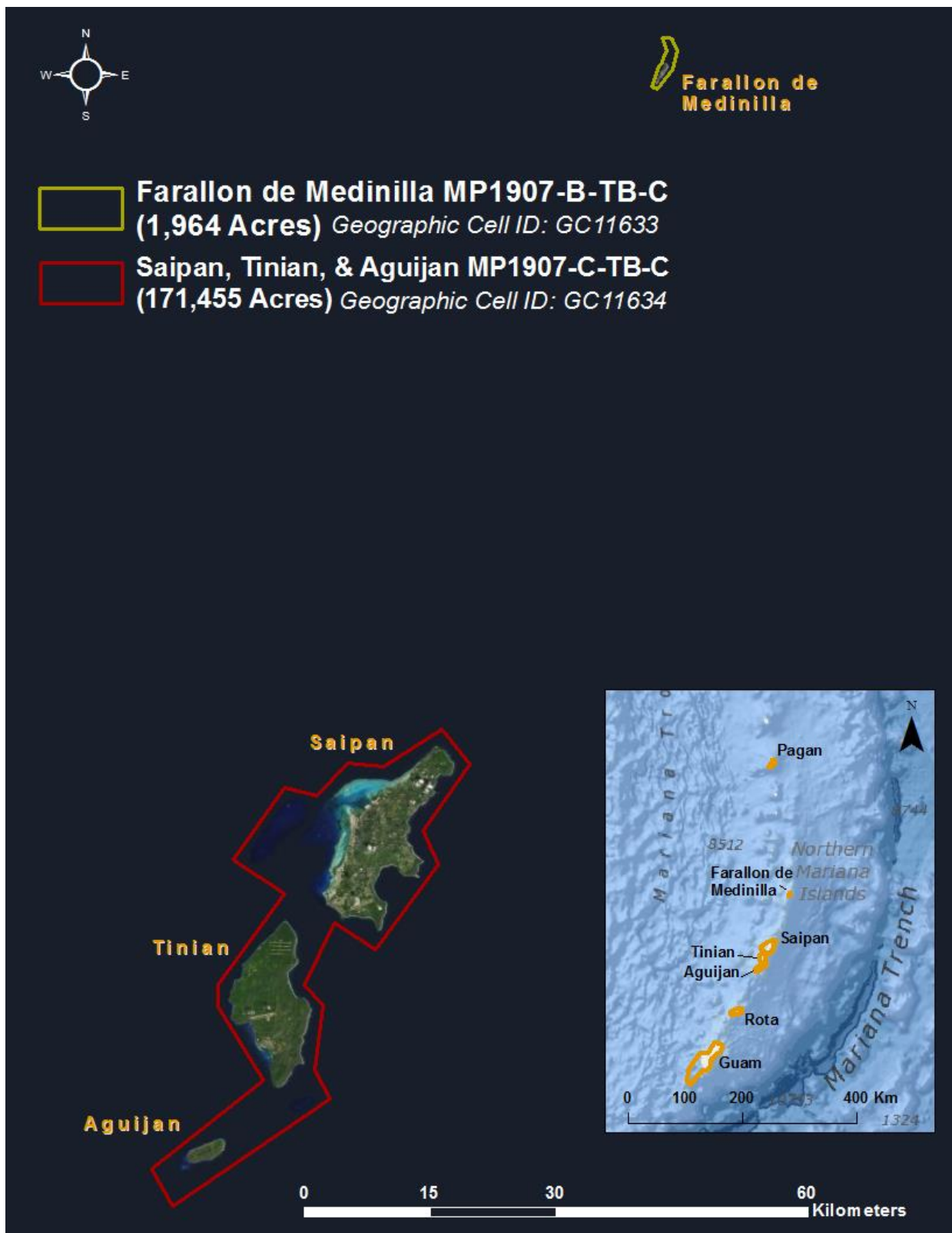


Figure 6: Location map of NOAA Typhoon Yutu Supplemental Shoreline Mapping areas of Aguijan, Tinian, Saipan, and Farallon de Medinilla.



Figure 7:: Location map of NOAA Typhoon Yutu Supplemental Shoreline Mapping site of Pagan.

Lidar Deliverables

Final topobathymetric Lidar deliverables for the Typhoon Yutu Guam and CNMI project areas were the final classified and tiled Lidar returns delivered in both ellipsoidal and orthometric heights, DZ ortho raster models, Standard Deviation raster models, topobathymetric bare earth DEMs, and supplemental shapefiles including bathymetric void polygons, flightline swaths, and mission coverage polygons. NV5 also provided several intermittent deliverables to NOAA in order to ensure project quality, consistency, and transparency in processing throughout the project. These additional intermittent deliverables included Quick-look Lidar coverage maps in GeoTIFF format to display bathymetric Lidar collection results. NOAA reviewed all QuickLook reports and approved each area for data processing or flagged each area to re-fly. SBETs were provided for each Lidar collection mission to ensure that NOAA is provided with all raw topobathymetric data.

Final topobathymetric lidar data was provided in 500 x 500 meter tiles, divided in two delivery blocks. The first delivery block covers the island of Guam with the second covering the four CNMI islands Alamagan, Anatahan, Sarigan, and Guguan. All associated shapefiles delineating tile grids were provided to NOAA with each delivery block, and as a final comprehensive tile index for the Guam and CNMI lidar project areas. Final lidar DZ Orthos were created in order to evaluate the line to line relative accuracy of the lidar data, and were delivered to NOAA in GeoTIFF format as well. Finally, FGDC compliant project metadata in .xml format were delivered with all final lidar data and derived deliverables.

DEM Deliverables

Woolpert, Inc. processed the final classified orthometric point cloud into the contracted DEM deliverables. All final tiled DEMs for the Guam area include orthometric heights from Vertical Datum GUVDO4, Geoid 12B, meters. All final tiled DEMs for the CNMI areas include orthometric heights from Vertical Datum NMVD03, Geoid 12b, meters.

The provided sets of tiled DEMs are enforced to the bathymetric void polygon so that areas lacking bathymetric bottom returns are set to “no data” to avoid false triangulation (interpolation from TIN’ing) across areas in the water with no bathymetric returns. All DEMs were delivered in ERDAS Imagine (*.img) format with a 1 meter cell size, tiled in a 5,000 x 5,000 meter grid. Void polygons used in DEM generation were provided in addition to a confidence layer. The confidence layer reports the standard deviation (in meters) of all ground and bathymetric bottom return points within each 1 meter cell, provided in ERDAS Imagine (*.img) format with a 1 meter pixel resolution, tiled in 500 x 500 meter grid.

Shoreline Deliverables

The NOAA Coastal Mapping Program (CMP) Projects MP1907A-TB-C, MP1907B-TB-C, MP1907C-TB-C, 1907D-TB-C, and GU1903-TB-C provide a highly accurate database of new digital shoreline data for the areas affected by Typhoon Yutu along the coastlines of Saipan, Tinian, Aguijan, Pagan, Rota, Guam and Farallon de Medinilla islands.

NOAA supplied NV5 Geospatial with previously acquired lidar derived Mean High Water (MWH) and Mean Lower-Low Water (MLLW) shorelines to be segmented, edited, and attributed. In addition, NV5 was responsible for compiling any shoreline features that were unable to be extracted from the lidar. These features were compiled photogrammetrically using satellite imagery from DigitalGlobe Inc provided by NOAA. NV5 received and mapped the shoreline from NOAA in five processing blocks each

identified with a Geographic Cell number and included all bays, inlets, and islands within 2000 feet of the coastline.

Successful completion of this project resulted in digital feature data of the coastal zone in support of the NOAA Nautical Charting Program (NCP) as well as geographic information systems (GIS) for a variety of coastal zone management applications. The project database consists of information measured and extracted from satellite photographs and metadata related to photogrammetric compilation. Base mapping was conducted in a digital environment using stereo softcopy photogrammetry and associated cartographic practices, supplemented with lidar derived Mean High Water (MHW) and Mean Lower Low Water (MLLW) data provided by NOAA.

Quality control tasks were conducted during all phases of project completion by an NV5 Geospatial senior mapping professional. The review process included analysis of aero-triangulation results and assessment of the identification and attribution of digital feature data within the subproject according to image analysis and criteria defined in C-COAST. The quality control process concluded with an inspection of topological connectivity within the project using ArcGIS 10.6 software. All project data was evaluated for compliance to CMP requirements.

Comparisons of the largest scale NOAA nautical charts with natural color satellite imagery and compiled project data resulted in creation of the Chart Evaluation File (CEF). The following nautical charts were used in the comparison process

Please see the enclosed shoreline mapping technical data reports for more detailed information regarding data acquisition and processing methodologies as well as the delivered Chart Evaluation Files (CEF)(Table 3) for additional accuracy assessments of the final shoreline deliverables.

Table 3: NOAA Shoreline Mapping Geographic Cell IDs

Project ID	Geographic Cell ID
MP1907A-TB-C	GC11632
MP1907B-TB-C	GC11633
MP1907C-TB-C	GC11634
MP1907D-TB-C	GC11635
GU1903-TB-C	GC11636

ACQUISITION

Leica Hawkeye 4X system installed in a Reims-Cessna F460 for the NOAA Typhoon Yutu Supplemental Mapping Topobathymetric Lidar Project. Photo provided by Woolpert, Inc.,



Planning

In preparation for data collection, NV5 provided Woolpert, Inc. the project area of interest to review and develop a specialized flight plan to ensure complete coverage of the Typhoon Yutu Supplemental lidar study area and to meet the USGS Lidar Base Specification 2.1 QL1 standards of 8 points per square meter as required for the topographic Lidar, while simultaneously acquiring bathymetric lidar to meet the National Coastal Map standards at 2 points per square meter. Acquisition parameters including orientation relative to terrain, flight altitude, pulse rate, scan angle, and ground speed were adapted to optimize flight paths and flight times while meeting all contract specifications. All Lidar data were acquired using a Chiroptera 4X(CH4X) sensor, with an additional Leica 40kHz deep bathymetric channel. The combination of these sensors is referred to as a Leica HawkEye 4X(HE4X) system.

Factors such as tidal conditions, satellite constellation availability, and weather windows must be considered during the planning stage. Any weather hazards or conditions affecting the flight were continuously monitored due to their potential impact on the daily success of airborne and ground operations. In addition, logistical considerations including private property access and potential air space restrictions. NOAA should note that the northwest corner of the Island of Guam is a restricted area and restricted air space so data sharing should be conducted appropriately.

Lidar Survey

The lidar survey was accomplished by Woolpert, Inc. using a Leica Chiroptera 4X (CH4X) laser system dually mounted with an additional Leica 40kHz deep bathymetric channel known as a Leica HawkEye 4X (HE4X) in a Reims-Cessna F406. The HawkEye 4X (HE4X) boasts a higher density point cloud in addition to excellent topographic, shallow water, and deep water performance. The green wavelength ($\lambda=532$ nm) laser is capable of collecting high resolution topography data, as well as penetrating the water surface with minimal spectral absorption by water. The Leica Chiroptera 4X (CH4X) contains an integrated NIR laser ($\lambda=1064$ nm) that adds additional topography data. The recorded waveform enables range measurements for all discernible targets for a given pulse. The typical number of returns digitized from a single pulse range from 1 to 15 for the Typhoon Yutu Supplemental Lidar project area. It is not uncommon for some types of surfaces (e.g., dense vegetation or water) to return fewer pulses to the lidar sensor than the laser originally emitted. The discrepancy between first return and overall delivered density will vary depending on terrain, land cover, and the prevalence of water bodies. All discernible laser returns were processed for the output dataset. Table 4 summarizes the settings used to yield an average topographic pulse density of ≥ 8 points/m² and an average bathymetric pulse density of ≥ 2 points/m² over the Typhoon Yutu Supplemental Lidar project area.

Table 4: Lidar specifications and survey settings

Lidar Survey Settings & Specifications			
Acquisition Dates	January 20, 2020-July 13, 2020		
Aircraft Used	Reims-Cessna F406		
Sensor	Leica		
Laser	Chiroptera 4X (NIR)	Chiroptera 4X (shallow green)	HawkEye 4X (HE4X)
Maximum Returns	15	15	15
Resolution/Density	To exceed 8 pulses/m ²	To exceed 2 pulses/m ²	To exceed 2 pulses/m ²
Nominal Pulse Spacing	0.35 m	0.71 m	0.71 m
Survey Altitude (AGL)	400-600 m	400-600 m	400-600 m
Survey speed	130 knots	130 knots	130 knots
Field of View	40°	40°	40°
Mirror Scan Rate	70 Hz	32-39 Hz	17-21 Hz
Effective Target Pulse Rate	300-450 kHz	140 kHz	40 kHz
Pulse Length	2.5 ns	2.5 ns	2.5 ns
Laser Pulse Footprint Diameter	88-132 cm	88-132 cm	88-132 cm
Central Wavelength	1064 nm	532 nm	532 nm
Pulse Mode	Continuous multipulse	Continuous multipulse	Continuous multipulse
Beam Divergence	0.25 mrad	0.25 mrad	0.25 mrad
Swath Width	291-437 m	291-437 m	291-437 m
Swath Overlap	15%	20%	20%
Intensity	16-bit	16-bit	16-bit
Accuracy	RMSE _z ≤ 15 cm	RMSE _z ≤ 15 cm	RMSE _z ≤ 15 cm

All areas were surveyed with an opposing flight line side-lap of $\geq 20\%$ ($\geq 40\%$ overlap) in order to reduce laser shadowing and increase surface laser painting. To accurately solve for laser point position (geographic coordinates x, y and z), the positional coordinates of the airborne sensor and the attitude of the aircraft were recorded continuously throughout the Lidar data collection mission. Position of the aircraft was measured twice per second (2 Hz) by an onboard differential GPS unit, and aircraft attitude was measured 200 times per second (200 Hz) as pitch, roll and yaw (heading) from an onboard inertial measurement unit (IMU). Two separate IMUs were collecting during the NOAA Typhoon Yutu acquisition due to the nature of the dually mounted sensor Hawkeye 4X set up. One IMU is in the main Chiroptera sensor head, which includes the topo channel (NIR) and shallow channel (green). The second IMU is contained within the deep channel sensor (green) installed over a second hatch in the aircraft. To allow for post-processing correction and calibration, aircraft and sensor position and attitude data are indexed by GPS time.

Table 5: Flight Missions by Date

Date	Flight #	Start Time (GPS Time)	End Time (GPS Time)
01/20/2020	1	225856	233835
01/22/2020	1	230307	010705 (+1)
01/23/2020	1	222049	025840 (+1)
01/24/2020	1	234849	021245 (+1)
01/30/2020	2	024802	030039 (+1)
02/04/2020	1	222644	025709 (+1)
02/05/2020	1	215051	011239 (+1)
02/06/2020	2	030423	224352
02/07/2020	1	220016	020413 (+1)
02/08/2020	1	214531	031522 (+1)
02/09/2020	1	222935	014404 (+1)
02/11/2020	3	011546	014011 (+1)
02/15/2020	1	003759	023552
06/19/2020	1	233655	024827 (+1)
06/21/2020	2	013916	030532 (+1)
06/26/2020	1	020219	055110
07/02/2020	1	024351	033635
07/13/2020	1	234344	003129 (+1)

**(+1) indicates next day*



Existing USACE Monument (NUTZ) Photo provided by Woolpert, Inc.



A Trimble R10 base station recording over an existing USACE Monument (NUTZ). Photo provided by Woolpert, Inc.

Ground Survey

Ground control surveys, including monumentation, aerial targets and ground survey points (GSPs), were conducted by Woolpert, Inc. to support the airborne acquisition. Ground control data were used to geospatially correct the aircraft positional coordinate data and to perform quality assurance checks on final lidar data and the satellite imagery used in editing the shoreline mapping deliverables.

Base Stations

GNSS base stations were used for collection of ground survey points on the Island of Guam using real time kinematic (RTK) survey techniques. Due to the distance of the CNMI from the single base station on Guam and their remoteness a precise point positioning (PPP) survey solution was used on the International Terrestrial Reference Frame (ITRF2014) (Table 7).

GNSS base station locations were selected with consideration for satellite visibility, field crew safety, and optimal location for GSP coverage. Woolpert, Inc. utilized two existing GNSS base stations for the Typhoon Yutu Supplemental Lidar project (Table 6, Figure 8).

Table 6: Base Station positions for the Typhoon Yutu Supplemental acquisition. Coordinates are on the NAD83 (MA11) datum, epoch 2010.00

Monument ID	Latitude	Longitude	Ellipsoid (meters)
PGUM	13° 28' 53.93566" N	144° 48' 12.93000" E	138.300
GUM2	13° 28' 53.92857" N	144° 48' 12.93512" E	138.345

Table 7: Base Station position for the Typhoon Yutu Supplemental acquisition. Coordinates are on the ITRF2014

Monument ID	Latitude	Longitude	Ellipsoid (meters)
RM1	19° 04' 35.10241" S	169° 55' 37.27601" W	88.102

Ground Survey Points (GSPs)

Ground survey points (GSPs), and bathymetric accuracy check points (BAPs) were collected by Woolpert, Inc. and provided to NV5 geospatial to be used in lidar calibration post-processing, and accuracy assessment (see Lidar Accuracy Assessments, page 27). Please also see the enclosed ground survey report (Yutu Supplemental Ground Control Report.pdf) for more information regarding the ground survey.

Aerial Targets

Aerial targets were placed throughout the shoreline project areas in order to geo-spatially correct the Digital Globe Inc. satellite imagery provided by NOAA to be able to reference during shoreline mapping. The targets were permanent features such as roadway turn arrows, stop sign bars, road strips, and other road markings, as well as corners of concrete platforms and corners of concrete sidewalks. Each target was precisely located using RTK points by Woolpert, Inc..



Land Cover Class

In addition to ground survey points, land cover class check points were collected throughout the study area to evaluate vertical accuracy. Vertical accuracy statistics were calculated for all land cover types to assess confidence in the lidar derived ground models across land cover classes (Table 8, see Lidar Accuracy Assessments, page 27).

Table 8: Land Cover Types and Descriptions

Land cover type	Land cover code	Example	Description	Accuracy Assessment Type
Short Grass	SH_GRASS		Maintained or low growth herbaceous grasslands	VVA
Tall Grass	TALL_GRASS		Herbaceous grasslands in advanced stages of growth	VVA
Forested	FOR		Forested areas dominated by deciduous species	VVA
Bare Earth	BARE, BE		Areas of bare earth surface	NVA
Urban	URBAN		Areas dominated by urban development, including parks	NVA

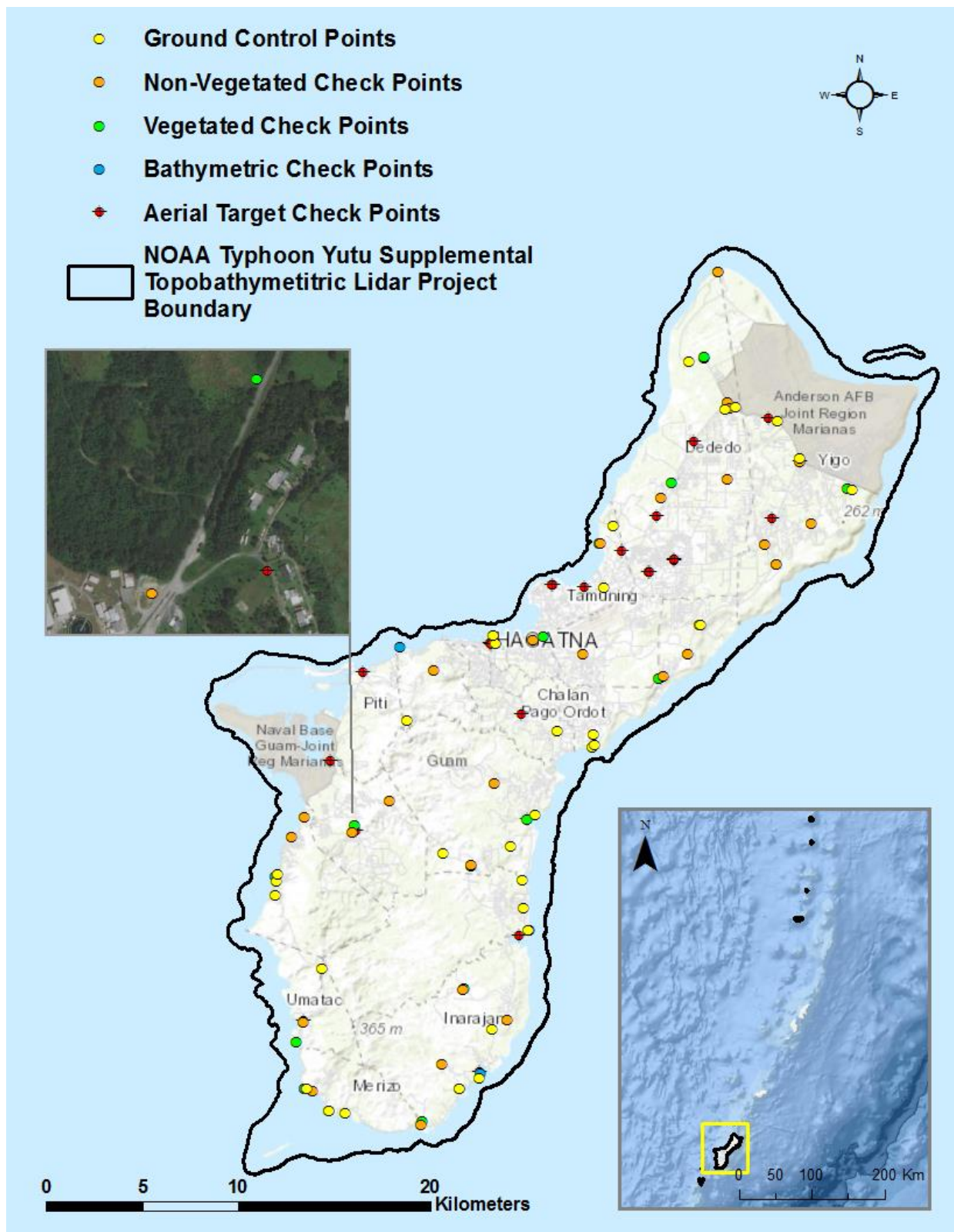


Figure 8: Ground survey location map

This 2 meter lidar cross section shows a view of the NOAA Typhoon Yutu Supplemental Mapping Topobathymetric Lidar land and bathy-scape, colored by point classification.

■ Ground
 ■ Default
 ■ Bathymetric Surface
 ■ Water Column
 ■ Water Surface
 ■ Submerged Object

Topobathymetric Lidar Data

Upon completion of data acquisition, Woolpert, Inc. initiated a suite of automated and manual techniques to process the data into the requested deliverables. Processing tasks included GPS control computations, smoothed best estimate trajectory (SBET) calculations, kinematic corrections, calculation of laser point position, sensor and data calibration for optimal relative and absolute accuracy, and lidar point classification (Table 9).

Bathymetric Refraction

Following final SBET creation for the Leica Chiroptera 4X and Hawkeye systems, Woolpert, Inc. used Leica Lidar Survey Studio (LSS) to calculate laser point positioning by associating SBET positions to each laser point return time, scan angle, and intensity. Leica LSS was used to derive a synthetic water surface to create a water surface model. Light travels at different speeds in air versus water and its direction of travel or angle is changed or refracted when entering the water column. The refraction tool corrects for this difference by adjusting the depth (distance traveled) and horizontal positioning (change of angle/direction) of the lidar data. All lidar data below the water surface model were classified as water column to correct for refraction. LSS then outputs the Lidar point cloud as classified LAS 1.4 files.

Table 9: ASPRS LAS classification standards applied to the Typhoon Yutu Supplemental dataset

Classification Number	Classification Name	Classification Description
1	Unclassified	Processed, but unclassified
2	Ground	Bare-earth ground
7	Noise	Noise (low or high; manually identified)
17	Bridge	Bridge decks
40	Bathymetric Bottom	Bathymetric point (e.g., seafloor or riverbed; also known as submerged topography)
41	Water Surface	Water's surface (sea/river/lake surface from topographic-bathymetric Lidar.
42-Synthetic	Derived Water Surface	Synthetic water surface location used in computing refraction at water surface
43	Submerged Feature	Submerged object, not otherwise specified (e.g., wreck, rock, submerged piling)
44	S-57 Object	International Hydrographic Organization (IHO) S-57 object, not otherwise specified
45	Water Column	Refracted returns not determined to be water surface or bathymetric bottom
46	Overlap Bathymetric Bottom	Denotes bathymetric bottom temporal changes from varying lifts, not utilized in the bathymetric point class
71	Adjacent Lift Unclassified	Adjacent lift Unclassified associated with areas of overlap bathy bottom where temporal bathymetric differences are present
72	Adjacent Lift Ground	Adjacent lift Ground associated with areas of overlap bathy bottom where temporal bathymetric differences are present
81	Adjacent Lift Water Surface	Adjacent lift Water Surface associated with areas of overlap bathy bottom where temporal bathymetric differences are present
85	Adjacent Lift Water Column	Adjacent lift Water Column associated with areas of overlap bathy bottom where temporal bathymetric differences are present
1-Overlap	Edge Clip	Unclassified points flagged as withheld. These are primarily "edge" points from the higher scan angle being removed.
1-Withheld	Withheld	Green sensor returns within topographic areas
139	Withheld Tail Clip	These are points from the start/end of lines overlapping in adjoining lifts where flight data is not consistent or necessary to create coverage
Original SOW classification scheme		Delivered in LAS files
Additional classification codes		Delivered in LAS files
Original SOW classification code not used		Not delivered in LAS files
Deleted points		Not delivered in LAS files

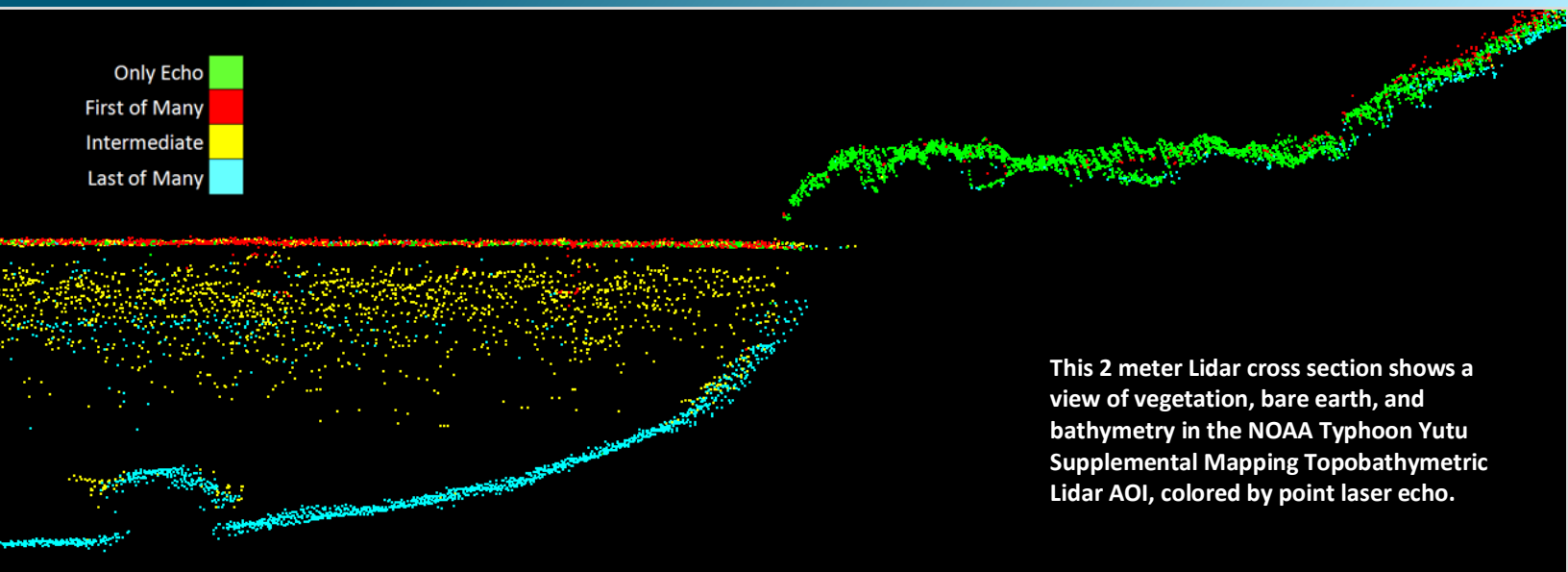
Lidar Derived Products

Because hydrographic laser scanners penetrate the water surface to map submerged topography, this affects how the data should be processed and presented in derived products from the Lidar point cloud. The following discusses certain derived products that vary from the traditional (NIR) specification and delivery format.

Topobathymetric DEMs

Bathymetric bottom returns can be limited by depth, water clarity, and bottom surface reflectivity. Water clarity and turbidity affects the depth penetration capability of the green wavelength laser with returning laser energy diminishing by scattering throughout the water column. Additionally, the bottom surface must be reflective enough to return remaining laser energy back to the sensor at a detectable level. Although the predicted depth penetration range of the Leica Hawkeye 4x (HE4X) is 2.7 Secchi depths on brightly reflective surfaces, it is typical to have no bathymetric bottom returns in turbid or non-reflective areas.

As a result, creating digital elevation models (DEMs) presents a challenge with respect to interpolation of areas with no returns. Traditional DEMs are “unclipped”, meaning areas lacking ground returns are interpolated from neighboring ground returns, with the assumption that the interpolation is close to reality. In bathymetric modeling, these assumptions are prone to error because a lack of bathymetric returns can indicate a change in elevation that the laser can no longer map due to increased depths. The resulting void areas may suggest greater depths, rather than similar elevations from neighboring bathymetric bottom returns. Therefore, a bathymetric void polygon was created to delineate areas outside of successfully mapped bathymetry. This shapefile was used to control the extent of the delivered clipped topobathymetric model and to avoid false triangulation across areas in the water with no returns. Insufficiently mapped areas were identified by triangulating bathymetric bottom points with an edge length maximum of 4.56 meters. This ensured areas with no bathymetric returns ($> 9 \text{ m}^2$), were identified as bathymetric data voids.



Bathymetric Lidar

An underlying principle for collecting hydrographic lidar data is to survey near-shore areas that can be difficult to collect with other methods, such as multi-beam sonar, particularly over large areas. In order to determine the capability and effectiveness of the bathymetric Lidar, certain parameters were considered; such as bathymetric return density and spatial accuracy.

Lidar Point Density

First Return Point Density

The acquisition parameters were designed to acquire an average first-return density of 8 points/m². First return density describes the density of pulses emitted from the laser that return at least one echo to the system. Multiple returns from a single pulse were not considered in first return density analysis. Some types of surfaces (e.g., breaks in terrain, water, and steep slopes) may have returned fewer pulses than originally emitted by the laser.

First returns typically reflect off the highest feature on the landscape within the footprint of the pulse. In forested or urban areas the highest feature could be a tree, building, or power line, while in areas of unobstructed ground, the first return will be the only echo and represents the bare earth surface.

The average first-return density of the Typhoon Yutu Supplemental Lidar project was 44.83 points/m² (Table 10).

Bathymetric and Ground Classified Point Densities

The density of ground and bathymetric bottom classified lidar returns were also analyzed for this project. Terrain character, land cover, and ground surface reflectivity all influenced the density of ground surface returns. In vegetated areas, fewer pulses may have penetrated the canopy, resulting in lower ground density. Similarly, the density of bathymetric bottom returns was influenced by turbidity, depth, and bottom surface reflectivity. In turbid areas, fewer pulses may have penetrated the water surface, resulting in lower bathymetric density.

The ground and bathymetric bottom classified density of Lidar data for the Typhoon Yutu Supplemental project was 13.11 points/m²(Table 10).

Table 10: Average Lidar point densities

Density Type	Point Density
First Returns	44.83 points/m ²
Ground and Bathymetric Bottom Classified Returns	13.11 points/m ²

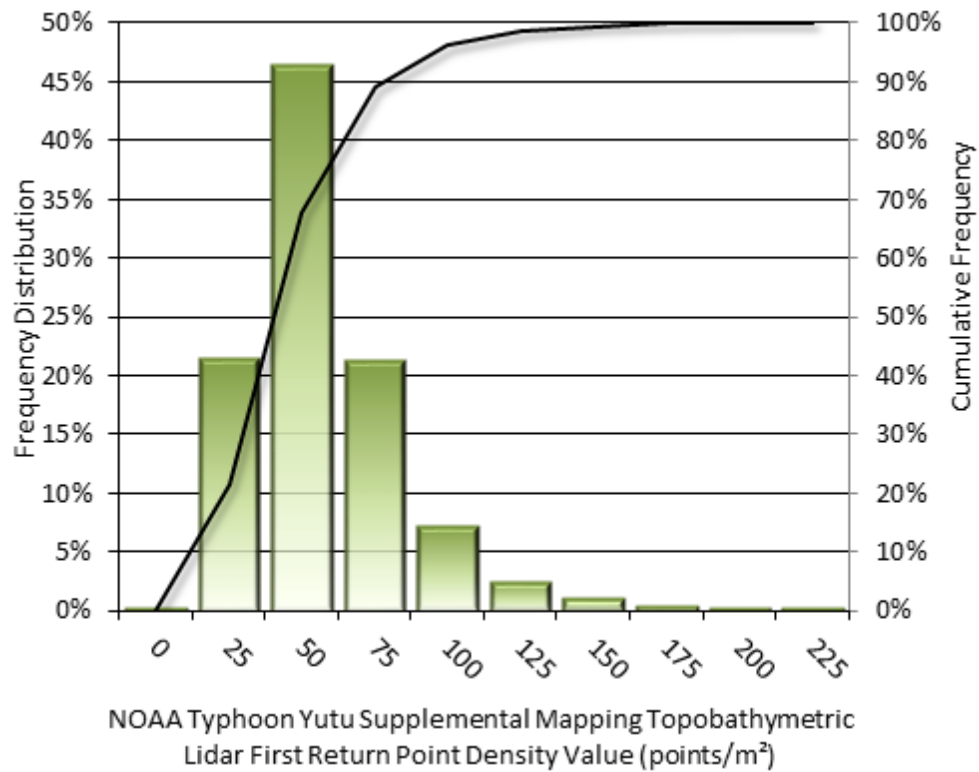


Figure 9: Frequency distribution of first return densities per 100 x 100 m cell

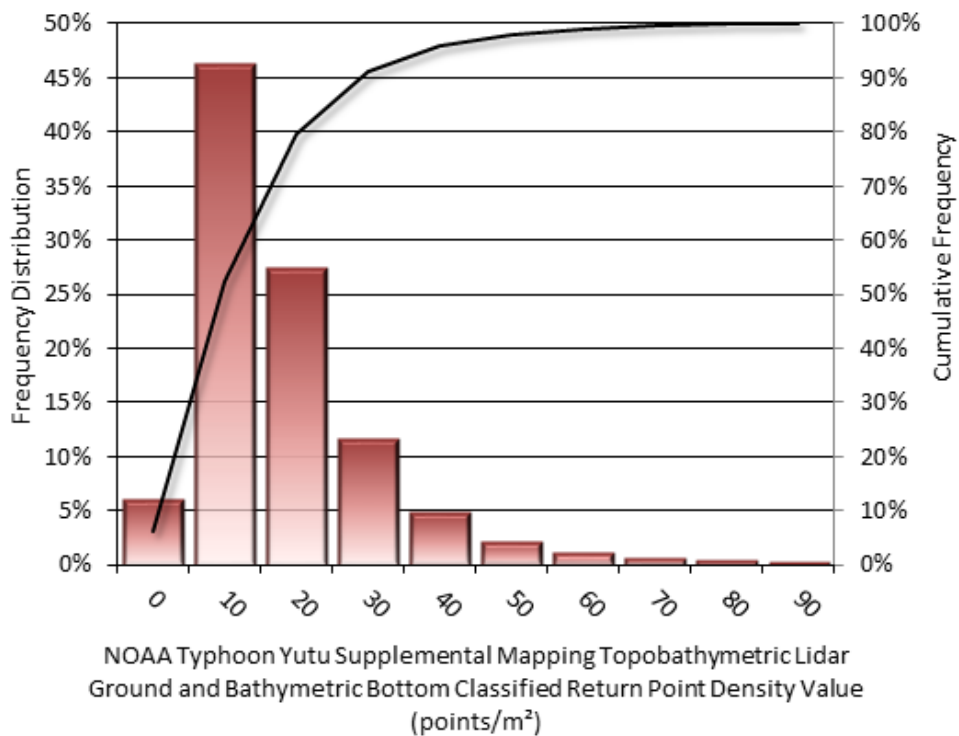


Figure 10: Frequency distribution of ground and bathymetric bottom classified return densities per 100 x 100 m cell

Lidar Accuracy Assessments

The accuracy of the Lidar data collection can be described in terms of absolute accuracy (the consistency of the data with external data sources) and relative accuracy (the consistency of the dataset with itself). See Appendix A for further information on sources of error and operational measures used to improve relative accuracy.

Lidar Non-Vegetated Vertical Accuracy

Absolute accuracy was assessed using Non-vegetated Vertical Accuracy (NVA) reporting designed to meet guidelines presented in the FGDC National Standard for Spatial Data Accuracy¹. NVA compares known ground check point data that were withheld from the calibration and post-processing of the Lidar point cloud to the triangulated surface generated by the classified Lidar point cloud as well as the derived gridded bare earth DEM. NVA is a measure of the accuracy of Lidar point data in open areas where the Lidar system has a high probability of measuring the ground surface and is evaluated at the 95% confidence interval ($1.96 * RMSE$), as shown in Table 11.

The mean and standard deviation (σ) of divergence of the ground surface model from ground check point coordinates are also considered during accuracy assessment. These statistics assume the error for x, y and z is normally distributed, and therefore the skew and kurtosis of distributions are also considered when evaluating error statistics. For the Typhoon Yutu Supplemental Lidar survey, 29 ground check points were withheld from the calibration and post-processing of the lidar point cloud, with resulting non-vegetated vertical accuracy of 0.100 meters, as compared to the classified LAS (Table 11 and Figure 11) and 0.092 meters against the bare earth DEM, with 95% confidence (Table 11 and Figure 12).

Absolute accuracy was also assessed using 32 ground control points. Although these points were used in the calibration and post-processing of the lidar point cloud, they still provide a good indication of the overall accuracy of the lidar dataset, and therefore have been provided in Table 11 and Figure 13.

¹ Federal Geographic Data Committee, ASPRS POSITIONAL ACCURACY STANDARDS FOR DIGITAL GEOSPATIAL DATA EDITION 1, Version 1.0, NOVEMBER 2014.
https://www.asprs.org/a/society/committees/standards/Positional_Accuracy_Standards.pdf.

Table 11: Absolute accuracy results

Absolute Vertical Accuracy			
	NVA, as compared to Classified LAS	NVA, as compared to Bare Earth DEM	Ground Control Points
Sample	29 points	29 points	32 points
95% Confidence (1.96*RMSE)	0.100 m	0.092 m	0.245 m
Average	0.001 m	-0.005 m	0.054 m
Median	-0.002 m	-0.008 m	0.032 m
RMSE	0.051 m	0.047 m	0.125 m
Standard Deviation (1 σ)	0.052 m	0.048 m	0.115 m

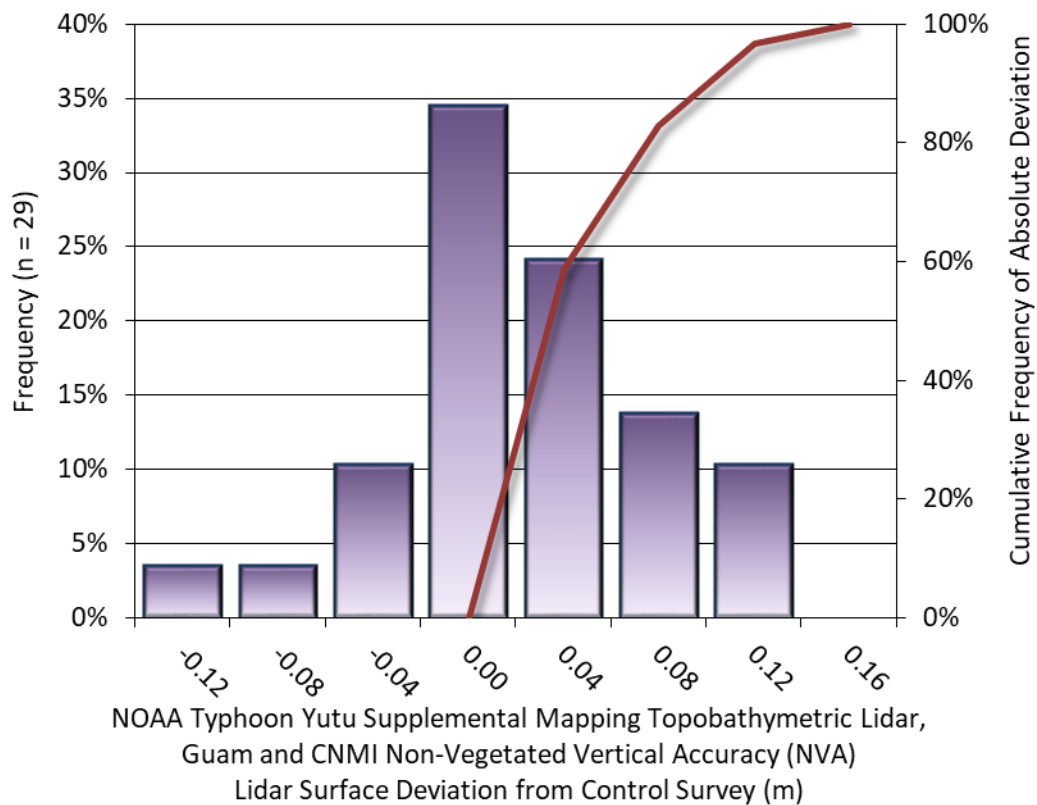


Figure 11: Frequency histogram for classified LAS deviation from ground check point values

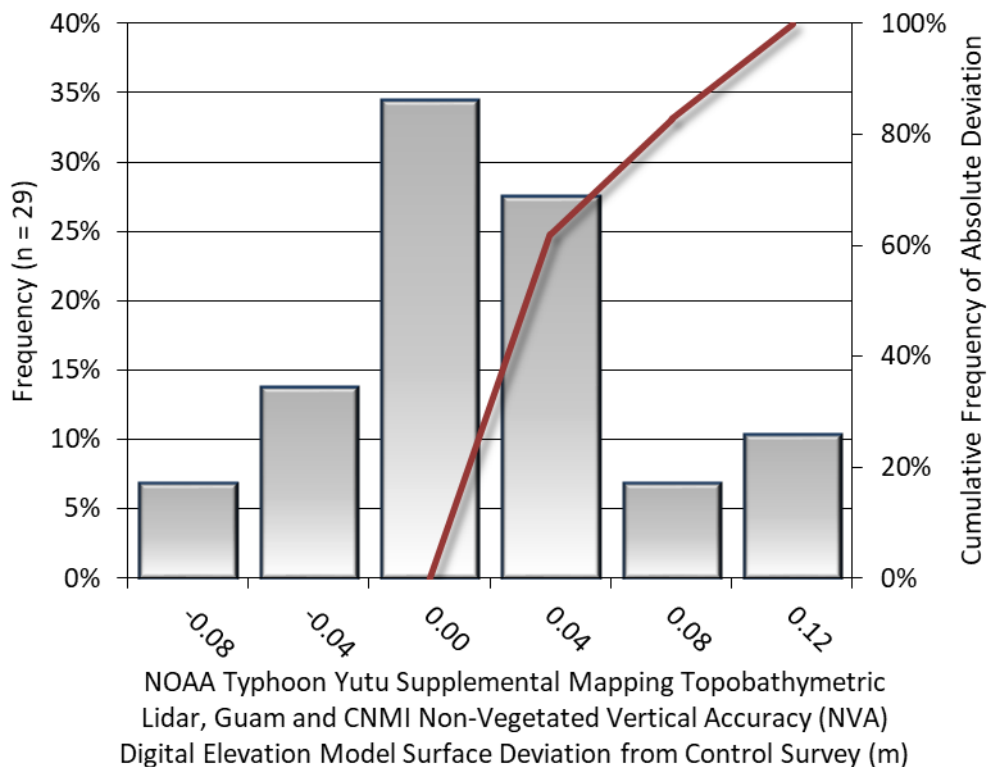


Figure 12: Frequency histogram for Lidar bare earth DEM deviation from ground check point values

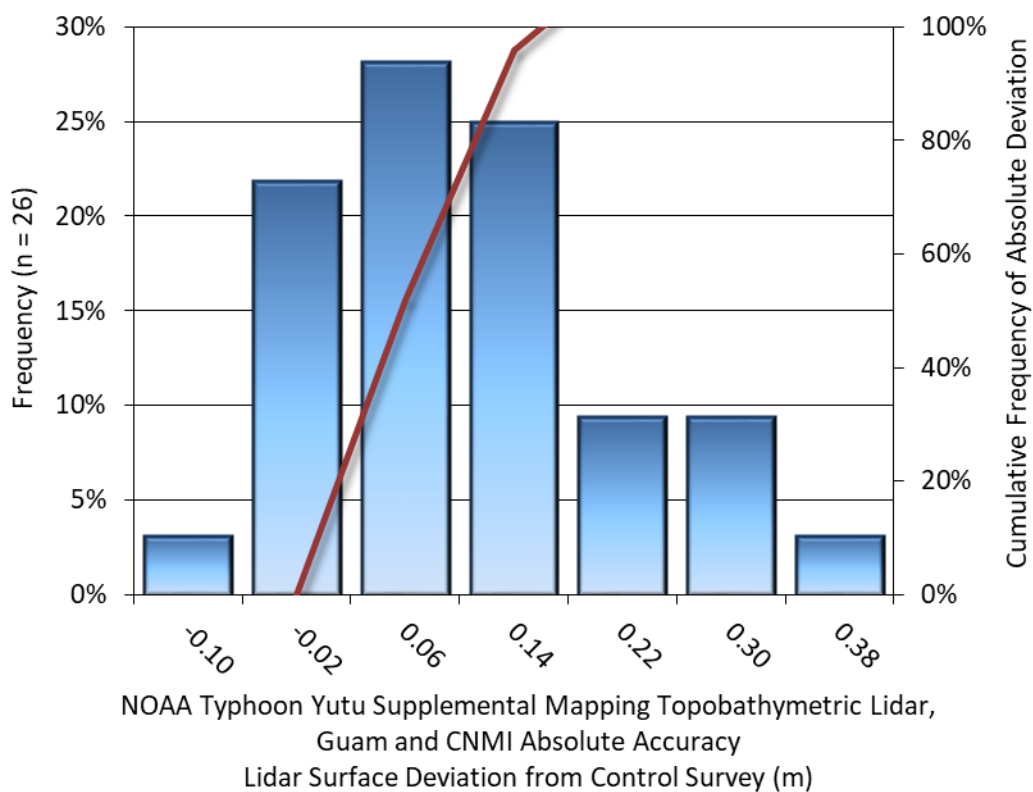


Figure 13: Frequency histogram for Lidar surface deviation ground control point values

Lidar Bathymetric Vertical Accuracies

Bathymetric (submerged) check points were also collected in order to assess the submerged surface vertical accuracy. Assessment of 6 submerged bathymetric check points resulted in a vertical accuracy of 0.233 meters (Table 12, Figure 14)

Table 12: Bathymetric Vertical Accuracy for the Typhoon Yutu Supplemental Topobathymetric Lidar Project

Bathymetric Vertical Accuracy (VVA)	
	Submerged Bathymetric Check Points
Sample	6 points
95% Confidence (1.96*RMSE)	0.233 m
Average Dz	0.096 m
Median	0.072 m
RMSE	0.119 m
Standard Deviation (1σ)	0.077 m

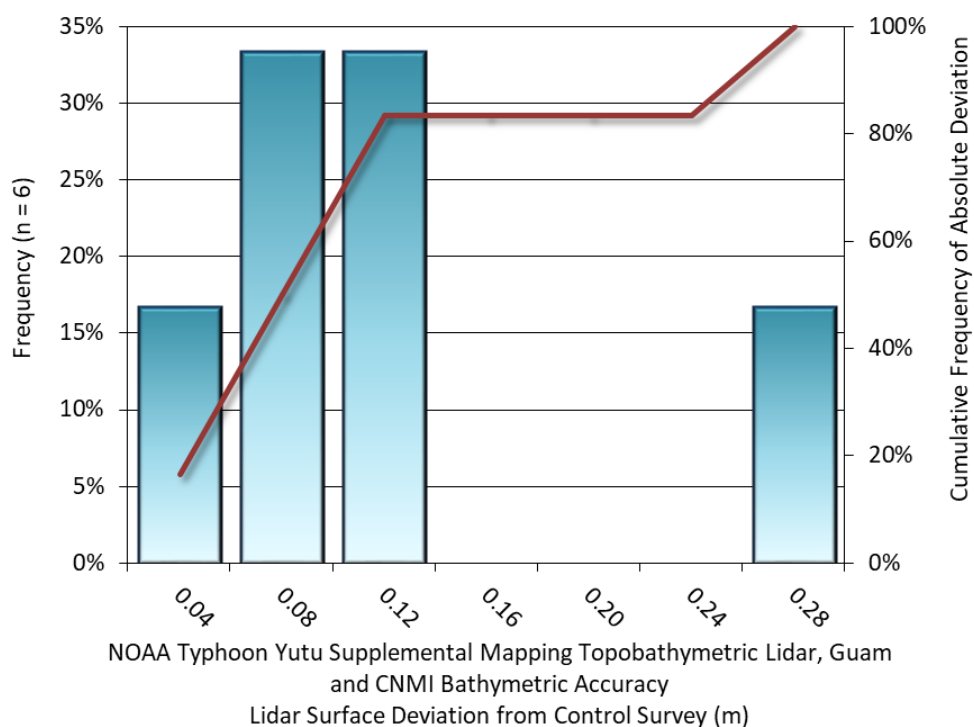


Figure 14: Frequency histogram for Lidar surface deviation from submerged check point values

Lidar Vegetated Vertical Accuracies

NV5 also assessed vertical accuracy using Vegetated Vertical Accuracy (VVA) reporting. VVA compares known ground check point data collected over vegetated surfaces using land class descriptions to the triangulated ground surface generated by the ground classified Lidar points. VVA is evaluated at the 95th percentile (Table 13, Figure 15, Figure 16).

Table 13: Vegetated Vertical Accuracy for the Typhoon Yutu Supplemental Topobathymetric Lidar Project

Vegetated Vertical Accuracy (VVA)		
	NVA, as compared to Classified LAS	NVA, as compared to Bare Earth DEM
Sample	13 points	13 points
Average Dz	0.142 m	0.168 m
Median	0.144 m	0.209 m
RMSE	0.170 m	0.192 m
Standard Deviation (1 σ)	0.098 m	0.097 m
95 th Percentile	0.269 m	0.284 m

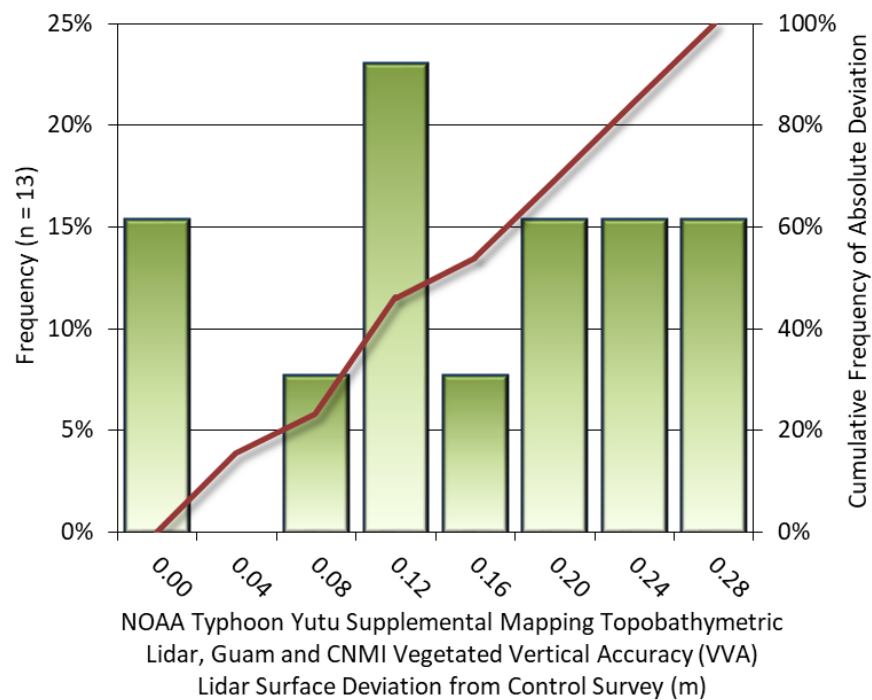


Figure 15: Frequency histogram for Lidar surface deviation from all land cover class point values (VVA) as compared against the ground classified LAS

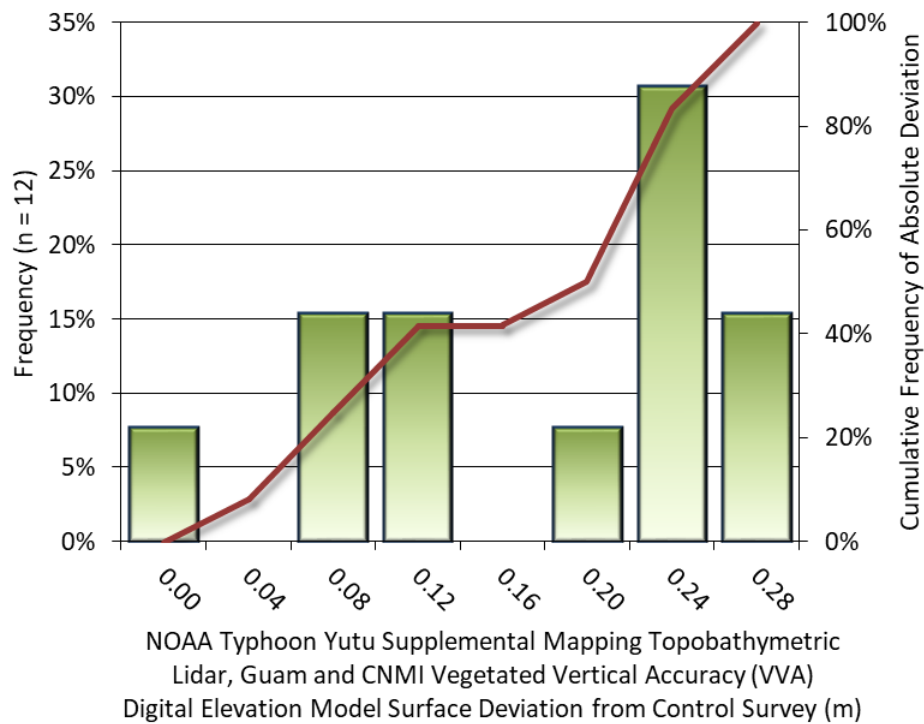


Figure 16: Frequency histogram for Lidar surface deviation from all land cover class point values (VVA) as compared against the bare earth DEM

Lidar Relative Vertical Accuracy

Relative vertical accuracy refers to the internal consistency of the data set as a whole: the ability to place an object in the same location given multiple flight lines, GPS conditions, and aircraft attitudes. When the Lidar system is well calibrated, the swath-to-swath vertical divergence is low (<0.10 meters). The relative vertical accuracy was computed by comparing the ground surface model of each individual flight line with its neighbors in overlapping regions. The RMSEDz line to line relative vertical accuracy for the Typhoon Yutu Supplemental Lidar project was 0.038 meters.

Lidar Horizontal Accuracy

Lidar horizontal accuracy is a function of Global Navigation Satellite System (GNSS) derived positional error, flying altitude, and INS derived attitude error. The obtained $RMSE_r$ value is multiplied by a conversion factor of 1.7308 to yield the horizontal component of the National Standards for Spatial Data Accuracy (NSSDA) reporting standard where a theoretical point will fall within the obtained radius 95 percent of the time. Due to the unique lidar acquisition of the NOAA Typhoon Yutu Supplemental Mapping Topobathymetric Lidar project area, the Guam flight missions and the CNMI flight missions were tested separately. Additionally, since the Leica Hawkeye 4X sensor has two IMUs, the horizontal accuracy was further split out by each sensor head (Chiroptera 4X shallow green and NIR, and the Hawkeye 4X deep green.)

For the Guam Lidar Chiroptera 4X (shallow green and NIR laser) acquisition, based on a maximum flying altitude of 600 meters, an IMU error of 0.006 decimal degrees, and a GNSS positional error of 0.015 meters, the horizontal accuracy at the 95% confidence level was 0.200 meters. For the Guam Lidar Hawkeye 4x (deep green laser) acquisition, based on a maximum flying altitude of 600 meters, an IMU error of 0.023 decimal degrees, and a GNSS positional error of 0.027 meters, the horizontal accuracy at the 95% confidence level was 0.750 meters.

For the CNMI Lidar Chiroptera 4X (shallow green and NIR laser) acquisition, based on a maximum flying altitude of 600 meters, an IMU error of 0.007 decimal degrees, and a GNSS positional error of 0.015 meters, the horizontal accuracy at the 95% confidence level was 0.132 meters. For the CNMI Lidar Hawkeye 4x (deep green laser) acquisition, based on a maximum flying altitude of 600 meters, an IMU error of 0.007 decimal degrees, and a GNSS positional error of 0.015 meters, the horizontal accuracy at the 95% confidence level was 0.230 meters.

Table 14: Horizontal Accuracy for Guam

Horizontal Accuracy		
	Chiroptera 4X (shallow green and NIR laser)	Hawkeye 4X (deep green laser)
$RMSE_r$	0.113 m	0.432 m
ACC_r	0.200 m	0.750 m

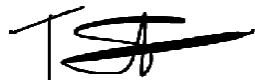
Table 15: Horizontal Accuracy for CNMI

Horizontal Accuracy		
	Chiroptera 4X (shallow green and NIR laser)	Hawkeye 4X (deep green laser)
$RMSE_r$	0.132 m	0.132 m
ACC_r	0.230 m	0.230 m

CERTIFICATIONS

NV5 Geospatial, Inc. provided lidar services for the Typhoon Yutu Supplemental project as described in this report.

I, Tucker Selko, have reviewed the attached report for completeness and hereby state that it is a complete and accurate report of this project.



Jun 25, 2021

Tucker Selko
Project Manager
NV5 Geospatial, Inc.

GLOSSARY

1-sigma (σ) Absolute Deviation: Value for which the data are within one standard deviation (approximately 68th percentile) of a normally distributed data set.

1.96 * RMSE Absolute Deviation: Value for which the data are within two standard deviations (approximately 95th percentile) of a normally distributed data set, based on the FGDC standards for Non-vegetated Vertical Accuracy (FVA) reporting.

Accuracy: The statistical comparison between known (surveyed) points and laser points. Typically measured as the standard deviation (sigma σ) and root mean square error (RMSE).

Absolute Accuracy: The vertical accuracy of Lidar data is described as the mean and standard deviation (sigma σ) of divergence of Lidar point coordinates from ground survey point coordinates. To provide a sense of the model predictive power of the dataset, the root mean square error (RMSE) for vertical accuracy is also provided. These statistics assume the error distributions for x, y and z are normally distributed, and thus we also consider the skew and kurtosis of distributions when evaluating error statistics.

Relative Accuracy: Relative accuracy refers to the internal consistency of the data set; i.e., the ability to place a laser point in the same location over multiple flight lines, GPS conditions and aircraft attitudes. Affected by system attitude offsets, scale and GPS/IMU drift, internal consistency is measured as the divergence between points from different flight lines within an overlapping area. Divergence is most apparent when flight lines are opposing. When the Lidar system is well calibrated, the line-to-line divergence is low (<10 cm).

Root Mean Square Error (RMSE): A statistic used to approximate the difference between real-world points and the Lidar points. It is calculated by squaring all the values, then taking the average of the squares and taking the square root of the average.

Data Density: A common measure of Lidar resolution, measured as points per square meter.

Digital Elevation Model (DEM): File or database made from surveyed points, containing elevation points over a contiguous area. Digital terrain models (DTM) and digital surface models (DSM) are types of DEMs. DTMs consist solely of the bare earth surface (ground points), while DSMs include information about all surfaces, including vegetation and man-made structures.

Intensity Values: The peak power ratio of the laser return to the emitted laser, calculated as a function of surface reflectivity.

Nadir: A single point or locus of points on the surface of the earth directly below a sensor as it progresses along its flight line.

Overlap: The area shared between flight lines, typically measured in percent. 100% overlap is essential to ensure complete coverage and reduce laser shadows.

Pulse Rate (PR): The rate at which laser pulses are emitted from the sensor; typically measured in thousands of pulses per second (kHz).

Pulse Returns: For every laser pulse emitted, the number of wave forms (i.e., echoes) reflected back to the sensor. Portions of the wave form that return first are the highest element in multi-tiered surfaces such as vegetation. Portions of the wave form that return last are the lowest element in multi-tiered surfaces.

Real-Time Kinematic (RTK) Survey: A type of surveying conducted with a GPS base station deployed over a known monument with a radio connection to a GPS rover. Both the base station and rover receive differential GPS data and the baseline correction is solved between the two. This type of ground survey is accurate to 1.5 cm or less.

Post-Processed Kinematic (PPK) Survey: GPS surveying is conducted with a GPS rover collecting concurrently with a GPS base station set up over a known monument. Differential corrections and precisions for the GNSS baselines are computed and applied after the fact during processing. This type of ground survey is accurate to 1.5 cm or less.

Scan Angle: The angle from nadir to the edge of the scan, measured in degrees. Laser point accuracy typically decreases as scan angles increase.

Native Lidar Density: The number of pulses emitted by the Lidar system, commonly expressed as pulses per square meter.

APPENDIX A - ACCURACY CONTROLS

Relative Accuracy Calibration Methodology:

Manual System Calibration: Calibration procedures for each mission require solving geometric relationships that relate measured swath-to-swath deviations to misalignments of system attitude parameters. Corrected scale, pitch, roll and heading offsets were calculated and applied to resolve misalignments. The raw divergence between lines was computed after the manual calibration was completed and reported for each survey area.

Automated Attitude Calibration: All data was tested and calibrated using TerraMatch automated sampling routines. Ground points were classified for each individual flight line and used for line-to-line testing. System misalignment offsets (pitch, roll and heading) and scale were solved for each individual mission and applied to respective mission datasets. The data from each mission were then blended when imported together to form the entire area of interest.

Automated Z Calibration: Ground points per line were used to calculate the vertical divergence between lines caused by vertical GPS drift. Automated Z calibration was the final step employed for relative accuracy calibration.

Lidar accuracy error sources and solutions:

Type of Error	Source	Post Processing Solution
GPS (Static/Kinematic)	Long Base Lines	None
	Poor Satellite Constellation	None
	Poor Antenna Visibility	Reduce Visibility Mask
Relative Accuracy	Poor System Calibration	Recalibrate IMU and sensor offsets/settings
	Inaccurate System	None
Laser Noise	Poor Laser Timing	None
	Poor Laser Reception	None
	Poor Laser Power	None
	Irregular Laser Shape	None

Operational measures taken to improve relative accuracy:

Low Flight Altitude: Terrain following was employed to maintain a constant above ground level (AGL). Laser horizontal errors are a function of flight altitude above ground (about $1/3000^{\text{th}}$ AGL flight altitude).

Focus Laser Power at narrow beam footprint: A laser return must be received by the system above a power threshold to accurately record a measurement. The strength of the laser return (i.e., intensity) is a function of laser emission power, laser footprint, flight altitude and the reflectivity of the target. While surface reflectivity cannot be controlled, laser power can be increased and low flight altitudes can be maintained.

Reduced Scan Angle: Edge-of-scan data can become inaccurate. The scan angle was reduced to a maximum of $\pm 20^\circ$ from nadir, creating a narrow swath width and greatly reducing laser shadows from trees and buildings.

Quality GPS: Flights took place during optimal GPS conditions (e.g., 6 or more satellites and PDOP [Position Dilution of Precision] less than 3.0). Before each flight, the PDOP was determined for the survey day. During all flight times, a dual frequency DGPS base station recording at 1 second epochs was utilized and a maximum baseline length between the aircraft and the control points was less than 13 nm at all times.

Ground Survey: Ground survey point accuracy (<1.5 cm RMSE) occurs during optimal PDOP ranges and targets a minimal baseline distance of 4 miles between GPS rover and base. Robust statistics are, in part, a function of sample size (n) and distribution. Ground survey points are distributed to the extent possible throughout multiple flight lines and across the survey area.

50% Side-Lap (100% Overlap): Overlapping areas are optimized for relative accuracy testing. Laser shadowing is minimized to help increase target acquisition from multiple scan angles. Ideally, with a 50% side-lap, the nadir portion of one flight line coincides with the swath edge portion of overlapping flight lines. A minimum of 50% side-lap with terrain-followed acquisition prevents data gaps.

Opposing Flight Lines: All overlapping flight lines have opposing directions. Pitch, roll and heading errors are amplified by a factor of two relative to the adjacent flight line(s), making misalignments easier to detect and resolve.